Available online at www.sciencedirect.com
SCIENCE DIRECT®
Journal of Non-Crystalline Solids 351 (2005) 922–928
JOURNAL OF NON-CRYSTALLINE SOLIDS
www.elsevier.com/locate/jnoncrysol

Low temperature–low hydrogen content silicon nitrides thin films deposited by PECVD using dichlorosilane and ammonia mixtures

G. Santana [1], J. Fandiño, A. Ortiz, J.C. Alonso *

Instituto de Investigación en Materiales, Universidad Nacional Autónoma de México, Cd. Universitaria, A.P. 70-360, Coyoacán 04510, Mexico D.F.

Received 4 June 2004; received in revised form 10 September 2004

Abstract

Low hydrogen content silicon nitride thin films have been obtained by direct plasma enhanced chemical vapor deposition at relatively low temperature (250 °C), using different NH_3/SiH_2Cl_2 flow rate ratios and RF powers. Deposition rates and refractive indices of the films, determined from ellipsometric measurements, were in the range from 13 to 19 nm/min, and from 1.763 to 2.35, respectively. Optical emission spectra of plasmas sustained at low RF powers (20–30 W) show a continuous band related to H_2, $SiCl_2$ emitting species and peaks related to N_2, SiH and SiH_2, indicating an incomplete decomposition of the SiH_2Cl_2 precursor. However, at high RF powers (60–80 W), the continuous band and most of the peaks related to molecular species are suppressed, meanwhile the other lines related to atomic species are intensified. According to infrared spectroscopy the samples deposited at high RF powers and a NH_3/SiH_2Cl_2 ratio equal to 2.5 present a low total content of hydrogen and are free of Si–H bonds. Current–voltage measurements revealed that these films have dielectric breakdown fields higher than 5 MV/cm and conductivities lower than 5×10^{-13} $(\Omega\,\mathrm{cm})^{-1}$, and are resistant to oxidation, even if they are immersed in water for long period of time.

PACS: 52.25.Mq; 52.70.Kz; 52.20.–j; 85.40.Sz

1. Introduction

Silicon nitride thin films are very important in the microelectronic and optoelectronic industries. This dielectric material combines optical, electrical, mechanical and chemical properties that make it ideal for fabricating a number of semiconductor devices [1,2]. Due to its electronic properties such as relatively wide band gap (4.0–5.0 eV), high dielectric breakdown field (10^6–10^7 V/cm), dielectric constant (4.0–7.5), along with its high density (up to 3.1 g/cm^3), mechanical strength, and hardness, and exceptional thermal and chemical stability, thin films of this material are ideal for applications such as electrical insulation in integrated circuits [3], gate dielectric layers in thin film transistors (TFTs) [4,5] and CMOS devices [6], barriers against ions (sodium) and water diffusion, and masks for selective oxidation of silicon [2], selective doping and KOH etching [7]. Additionally, since silicon nitride films present very low absorption losses in the visible and infrared regions, and its index of refraction can be varied continuously over a wide range (1.7–3.0) by changing its composition, they are also very attractive for applications in thin film waveguides with desired characteristics of fiber match and compactness, and other integrated optical devices

* Corresponding author. Tel.: +52 56224606; fax: +52 56161251.
E-mail address: alonso@servidor.unam.mx (J.C. Alonso).
[1] Permanent address: IMRE Universidad de la Habana, 10400, Cuba.

0022-3093/$ - see front matter © 2005 Elsevier B.V. All rights reserved.
doi:10.1016/j.jnoncrysol.2005.02.007

[8,9], and anti-reflecting and passivating coatings in silicon solar cells [10]. High quality silicon nitride films are usually prepared at high temperatures (700–800 °C) by different thermally assisted chemical vapor deposition using mixtures of silane (SiH_4) and/or dichlorosilane ($SiCl_2H_2$) and ammonia (NH_3) [11,12]. However, the advance of amorphous silicon technology and the continuous development of the microelectronic industry toward integrated circuits (IC) with nano-scale features, has demanded important reductions in the processing temperatures of silicon-compound thin films [13–16].

This requirement has widespread the use of diverse plasma enhanced chemical vapor deposition (PECVD) processes for depositing at low temperatures high quality silicon nitride films, such as electron cyclotron resonance [17,18], remote-PECVD [5,14,19], inductively coupled (IC) PECVD [16,20], and the conventional parallel plate-capacitive coupled PECVD [6,10,12,21–24]. It should be mentioned that the latter PECVD version has continuously been of great interest because it has been largely studied and scaled-up to mass production dimensions in the production lines [21,25]. The most common precursors for these silicon nitride PECVD processes have been SiH_4 and NH_3. One of the advantages of using this mixture is the relatively high film deposition rates that can be achieved due to the easy decomposition of the SiH_4. However, one of the main troubles found when using these mixtures is the incorporation of large amounts of hydrogen in the films, in the form of Si–H and N–H bonds, which in fact are generically named hydrogenated amorphous silicon nitride (a-SiN_x:H). In a great number of applications, the hydrogen incorporated into the film matrix is undesirable. For example, Si–H bonds cause severe reliability problems in the performance of metal–insulator–semiconductor (MIS) devices and TFTs incorporating a-SiN_x:H thin films [5,17]. On the other hand N–H bonds are reported to be responsible for absorption problems in a-SiN_x:H layers for integrated optics applications [26]. Other problem found in PECVD a-SiN_x:H films deposited at low temperatures is that they possess a porous structure which allows moisture (H_2O from the ambient) percolation into their network with the resultant oxidation of the entire film [24].

The use of halogenated silicon precursors like dichlorosilane (SiH_2Cl_2), which contains less H atoms per Si atom than the SiH_4 molecule, has been proposed recently as a good alternative to reduce hydrogen incorporation in PECVD films deposited at 350–380 °C, without reducing significantly the deposition rates compared with the corresponding thermal CVD process [11,12,20]. However, the reduction of substrate temperatures below 300 °C, maintaining or even improving the physical and chemical properties of the silicon nitride films is a permanent challenge for materials science researchers.

In this work, we investigate the properties and stability of silicon nitride thin films prepared by direct PECVD at 250 °C from SiH_2Cl_2 and NH_3 mixtures. We used two different groups of deposition conditions in order to exploit the advantages of dichlorosilane to produce films with low hydrogen concentration. First, the ammonia to dichlorosilane flow ratio was varied keeping the rest of the working parameters at constant values, then we studied the influence of the RF plasma power on the films properties.

2. Experimental

The silicon nitride films were prepared using a conventional PECVD system, with parallel plates 150 cm^2 in area, 1.5 cm apart, and activated by a 13.56 MHz RF signal. The films were deposited on n-type (1 0 0) silicon slices having a resistivity of 200 and 1–0.2 Ω cm, for structural and electrical characterization, respectively. The low resistivity substrates were subjected to an standard RCA cleaning procedure and were also etched in diluted hydrofluoric acid (5% HF) immediately before loading them into the deposition chamber, in order to remove the native oxide present on the silicon surface. Dichlorosilane and ammonia, with argon as the diluent gas, were used as precursor gases. The deposition pressure and substrate temperature were kept constant during all the experiments, at 350 mTorr and 250 °C, respectively. In order to obtain silicon nitride thin films with various compositions, the flow ratio of NH_3 to SiH_2Cl_2 ($R = [NH_3]/[SiH_2Cl_2]$), and the applied RF plasma power were varied according to the designed processes shown in Table 1. In both cases only one parameter at a time was changed, keeping all the rest at constant values. In the first set of experiments the RF power was 30 W meanwhile R was varied from 1.0 to 10. In the second set of experiments the value of R was fixed at a value selected from the previous experiments (2.5) and the RF power was varied from 20 to 80 W. The Ar flow rate was kept constant at 50 sccm in all the experiments.

A Gaertner L117 Ellipsometer equipped with a He–Ne laser ($\lambda = 632.8$ nm) was used to measure the refractive index and thickness of the films. The bonding structure of the films was analyzed by means of a Fourier transformed infrared (FTIR) spectrometer (Nicolet-210). Optical emission spectroscopy (OES) in

Table 1
Deposition conditions

Process	Pressure (mTorr)	Temperature (°C)	$R = NH_3/SiH_2Cl_2$	RF power (W)
1	350	250	1–2.5–5–10	30
2	350	250	2.5	20–30–40–60–80

the wavelength range of 270–700 nm was assessed with the aid of an automated system based on an ORIEL 77250 monochromator, an RCA IP28 photomultiplier, a Keithley 240 A high voltage source and a Keithley 619 electrometer.

For the electrical conductivity measurements MIS devices were fabricated, incorporating the deposited silicon nitride films, 200 nm thick, 1.2 mm in diameter aluminum disks were thermally evaporated onto the films. The pressure during the thermal evaporation of aluminum was maintained at about 10^{-6} Torr. In–Ga eutectic was manually applied on the back surface of the low resistivity silicon substrates to form ohmic contacts. The bulk electrical characteristics (intrinsic breakdown) of all the silicon nitride films (except those chemically unstable and/or with undesirable or bad structural characteristics) were studied by applying and increasing the voltage, in steps of 0.5 V s^{-1}, through a gate probe (~100 μm tip) and measuring the current density versus electric field (J versus E) characteristics until breakdown. For these experiments we used a Keithley 230 programmable voltage source and a Keithley 485 autoranging picoammeter, both managed with the aid of a PC program written specifically for this purpose. Measurements were repeated on several similar devices to ascertain the consistency and reproducibility of the results.

3. Results and discussion

Fig. 1 shows the deposition rate and refractive index versus R for silicon nitride thin films deposited with an RF power of 30 W. Both, deposition rate and refractive index decrease with the increase in the ammonia concentration. This behavior is similar to that observed for silicon nitride films deposited by LPCVD and inductively coupled plasma-CVD (ICP-CVD) from dichlorosilane and ammonia, although our deposition rates were relatively higher (in the range from 12 to 20 nm/min) [11,20]. The decrease in the deposition rate as R increases indicates that under the used experimental conditions the growth of these films is limited by the partial pressure of the Si precursor gas (dichlorosilane), which decreases with NH_3 dilution. The decrease in the refractive index of the a-SiN_x films with NH_3 dilution (Fig. 1(b)) can be associated with an increase in the incorporation of nitrogen atoms in the silicon nitride network, which changes the composition of the deposited film from silicon rich to nitrogen rich. As Fig. 1(b) shows, for $R = 1$ the refractive index value (2.35) is higher than that corresponding to stoichiometric silicon nitride (2.0), indicating a silicon rich film. For $R > 1$ the refractive index decreases as R increases, taking values lower than 2.0, which is indicative of nitrogen rich films.

Fig. 2 shows IR absorption spectra for films deposited under the different ammonia/dichlorosilane ratios. The spectra of samples deposited with $R \geqslant 2.5$ show the principal absorption bands related to Si–N stretching and breathing vibration modes, which are centered between 850 and 890 cm^{-1}, and 480 and 500 cm^{-1}, respectively, and peaks located at 3346 cm^{-1} and 1170 cm^{-1}, which can be associated to N–H stretching and bending modes, respectively [19,20,24–28]. The increase in the incorporation of N–H bonds as R increases is well expected since the concentration of NH_x, NH_x^* ($x = 1, 2$) and related species generated in the plasma,

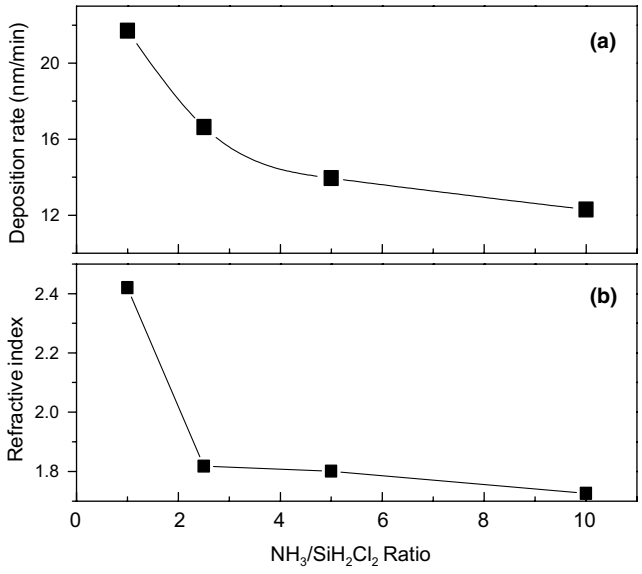

Fig. 1. Deposition rate and refractive index as a function of gas ratio R, for samples of process 1.

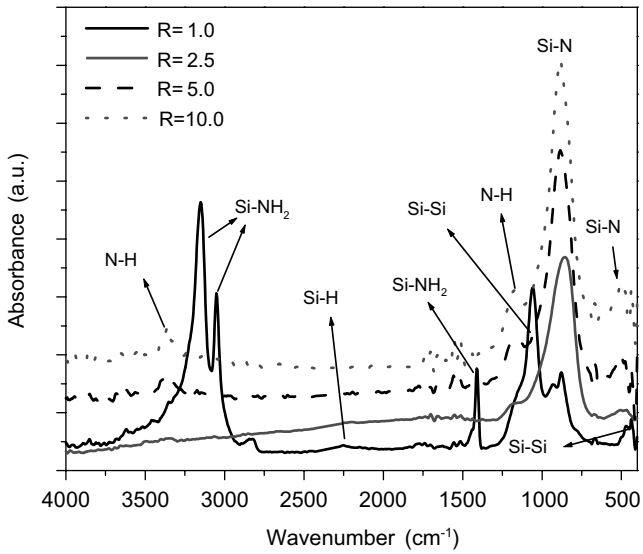

Fig. 2. FTIR spectra of process 1 samples deposited with an applied RF power of 30 W and different NH_3/SiH_2Cl_2 ratios.

which are available to be incorporated in the films, increases as the NH_3 flow rate rises. The IR spectrum of the film deposited with $R = 1$ looks quite different to the spectra of the other samples. In this spectrum, the absorption peak related to the Si–N stretching mode appears diminished, and some new dominant features can be observed at 3160, 3040, 1418, 1053, and 922 cm^{-1}, as well as other small peaks at 2840 and 2266 cm^{-1}. Additionally, the absorption peak with the lowest frequency instead of appearing around 500 cm^{-1}, as in the spectra of films deposited with $R \geqslant 2.5$, it appears at 421 cm^{-1}. The peaks at 3160, 3040, and 1418 cm^{-1} can be related to Si–NH_2 vibrations, meanwhile the peaks at 1053 and 421 cm^{-1} can be associated to Si–Si vibrational modes [11,24,27,29]. On the other hand the peak at 2266 cm^{-1} may be related to vibrations of SiH_2 and/or chlorosilane species such as Cl_3Si–H, meanwhile the peak at 922 cm^{-1} may also related to SiH_2 vibrations [30]. The peak at 2840 cm^{-1} could not be identified.

The presence of Si–Si bonds in the film deposited with $R = 1$ (30 W), as detected through the corresponding absorption peaks, suggest a silicon rich composition for this film, which is consistent with its high refractive index (2.35). On the other hand, the presence of IR features related to species such as NH_2, SiH_2, Cl_3Si–H, in the spectrum of this film indicates that under these conditions there is no complete decomposition of the SiH_2Cl_2 and NH_3 precursor molecules. As it will be shown below, this conclusion is consistent with the results obtained from the OES experiments. For $R = 2.5$, both, the IR spectrum features and refractive index value (around 1.8) of the film are the closest to those reported for stoichiometric silicon nitride films. The lowest concentration of N–H bonds incorporated in the film was also obtained under this value of R. Based on these results, the $R = 2.5$ value was chosen to proceed with the next set of experiments in order to produce silicon nitride thin films with characteristics as near as possible to the Si_3N_4 films, and with a minimal amount of N–H bonds incorporated.

Fig. 3 shows the influence of the RF power on the deposition rate and refractive index of films deposited with $R = 2.5$. The growth rate increases asymptotically toward a saturation value when the RF power increases. This can be explained by assuming that the increase in the effective power gives rise to a more effective decomposition of the dichlorosilane molecules, which increases the density of Si precursors that contribute to film growth. Based on this assumption, saturation of the growth rate is well expected at high powers where the exhaustion of the non-dissociated silicon species start to occur, and the growth kinetic switches from reactive species density-limited to surface chemical reactions-limited.

The increase in the refractive index as the RF power rises is indicative of silicon enrichment of the films. This

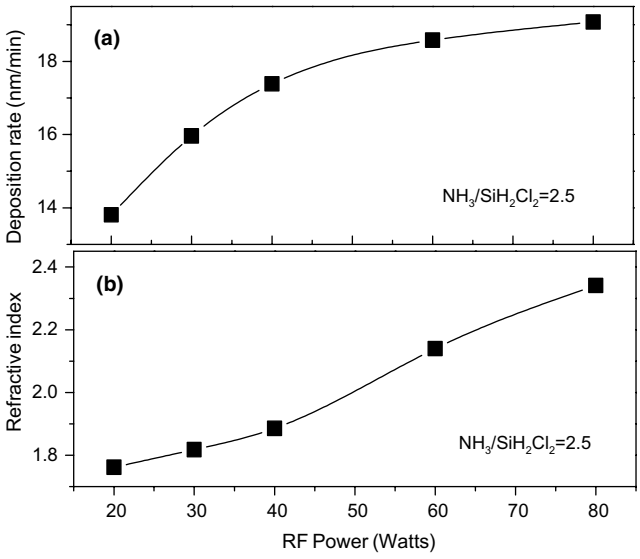

Fig. 3. Deposition rate and refractive index as a function of the applied RF power for samples of process 2.

behavior is also associated to the fact that as the RF power rises, more condensable silicon species (those that form the solid film) are generated from the decomposition of the SiH_2Cl_2 precursor and incorporated in the film.

In order to have more information on the nature of the reacting species generated under the different plasma powers, in situ optical emission spectroscopy was used to study the plasma. Fig. 4 shows the spectra of films deposited at 20, 30, 60 and 80 W. As can be seen from this figure, the emission spectrum for the lowest value of RF power (20 W) shows predominantly a continuum band extending from 250 to 425 nm, and other lines in

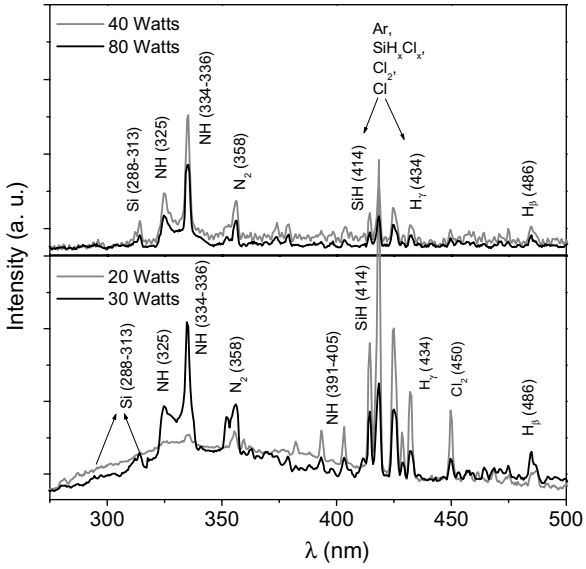

Fig. 4. OES spectrum of the plasma for different applied RF powers for samples of process 2.

the region from 410 to 500 nm. The continuous band can be identified as the superposition of two well-known continuums; one due to emission from H_2 molecules and another due to $SiCl_2$ molecules and SiH_xCl_y species [31,32]. The other intense lines are identified with species such as SiH (414 nm), Cl (425 nm), Cl_2 (450 nm), and atomic H (434, 486 nm). Lines corresponding to emission from Si (313 nm), NH (325 and 334 nm) species, and N_2 (358 nm) are also observed in the spectrum obtained at 20 W, but their intensity is very low. The whole characteristics of this spectrum indicate that at this low plasma power the decomposition of the $SiCl_2H_2$ is predominantly into $SiCl_2$ and H_2 molecules and that the NH_3 molecules are incompletely decomposed too. Although all these radicals can take part in reactions that form the film, the low deposition rates obtained in this case can be explained as a consequence of a low reactivity of the partially saturated $SiCl_2$ and N_2 species, and the low concentration of the more reactive unsaturated Si and NH species. As the power increases to 30 W the intensity of the lines related to NH, N_2, and Si, increases, and the intensity of the continuum band and that of the SiH, H, Cl, and Cl_2 lines decreases, indicating that under these conditions there is a better decomposition of both, $SiCl_2H_2$ and NH_3 molecules. The increase in the intensity of the Si and N_2 lines is consistent with the increase in the refractive index as the power increases. This is because an increase in the Si radicals concentration implies that more Si atoms are incorporated in the film, meanwhile the formation of volatile N_2 will inhibit the incorporation of nitrogen in the film. For plasma powers higher than 30 W, the continuous band related to H_2, $SiCl_2$ and SiH_xCl_y tends to disappear, and the intensity of most of the other lines, except that of Si decreases. The behavior of the intensity of the most important emission lines as a function of plasma powers up to 80 W, is depicted in Fig. 5. As can be seen from this figure the intensity of the lines related to SiH, NH, H and Cl_2 decreases as the plasma power increases from 30 to 80 W. This suggests that at high powers the formation of H and Cl radicals in high concentrations favors the mutual elimination of H and Cl, very probably due to the formation of HCl, and lowers the probability of Si–H and N–H bonds formation in the film, since the nitrogen radicals are energetically favored to form more stable Si–N bonds.

The FTIR spectra of films deposited at the different applied RF powers are shown in Fig. 6. A decrease in the NH bonds concentration is observed as the applied power rises. This result is consistent with the increase in the refractive index behavior shown in Fig. 3, if we realize that less nitrogen and hydrogen incorporated in the film produces a silicon richer composition, and a less porous structure. The peak related to the Si–H stretching mode (2160–2220 cm^{-1}) also decreases as the applied power increases and for 60 and 80 W it is not observed, indicating that its concentration is below the limit of detection (1%) [15]. This result is clarified in the insert of Fig. 6, where a close-up of the corresponding segment of the spectra is shown.

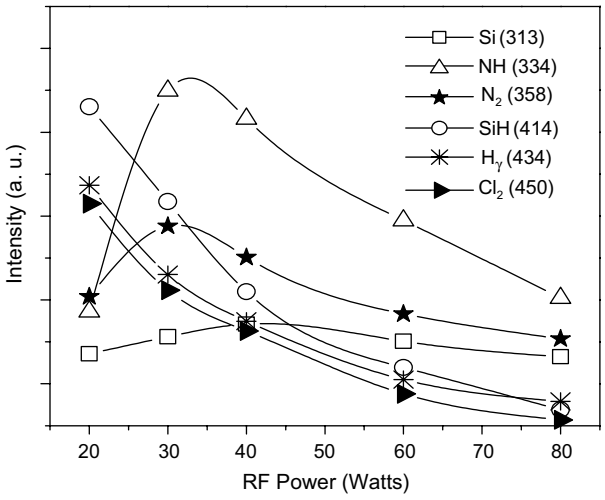

Fig. 5. Emission intensities of some excited species in SiH_2Cl_2/NH_3 plasmas as a function of the RF power.

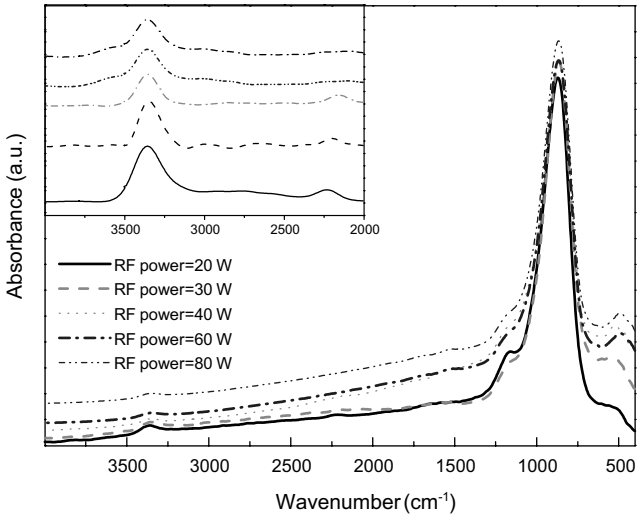

Fig. 6. FTIR spectra of samples deposited with $NH_3/SiH_2Cl_2 = 2.5$ and different applied RF powers. The inset shows that the IR absorption bands corresponding to N–H (3346 cm^{-1}) and Si–H (2150 cm^{-1}) bonds are diminished as the RF power increases.

The fact that most of the hydrogen present in the SiN_xH_y films is bonded to nitrogen (instead of silicon) is a consequence of the near-complete decomposition of dichlorosilane-based precursors. This assumption is confirmed by the emission spectra of Fig. 4, where it can be seen that the SiH related peak (414 nm) vanishes for high RF power while the emission corresponding to NH radicals (325 and 330 nm) still appears. Our films were chlorine-free up to the FTIR detection limit.

Higher values of the applied RF power were not used, because it increases the ion flux to the substrate, producing damage in the films by ion bombardment.

The concentrations C_i of Si–H and N–H bonds in the films were evaluated by integrating the corresponding peaks in the FTIR spectra, using the formula

$$C_i = K_i \int a(\omega)\,\mathrm{d}\omega,$$

where $a(\omega)$ is the absorption constant as a function of the wavenumber ω for the peak i (Si–H or N–H), and K_i is an empirical constant [28]. For the peaks in question we used the following values $K_{\mathrm{Si-H}}$ (2150 cm^{-1}) = $7.1\times10^{16}\ \mathrm{cm}^{-1}$, $K_{\mathrm{N-H}}$ (3350 cm^{-1}) = $8.2\times10^{16}\ \mathrm{cm}^{-1}$ [28,33]. Fig. 7 shows the plot of the N–H + Si–H bonds concentration in the films as a function of the applied power. As can be seen the total concentration of hydrogen decreases as the power increases. For high powers (60 and 80 W) concentration of hydrogen is only due to N–H bonds and it is below $1\times10^{22}\ \mathrm{cm}^{-3}$. The inset of Fig. 7 shows that the decrease in the hydrogen concentration as the power increases is accompanied by a linear decrease in the Si–N stretching frequencies. This behavior is similar to that found for silicon nitride films deposited by RPECVD from SiH_4/NH_3 mixtures [27,28].

Chemical stability of these films was tested by immersing them in water for 170 h. After this process no change was observed in the FTIR spectra, neither in the refractive index, which allows us to conclude that all the films under such conditions were chemically stable. This is an important achievement for applications of these films in the microelectronics, since one of the major problems found in plasma-deposited low temperature silicon nitride films is that they suffer a post deposition oxidation when exposed to the ambient moisture, which degrade their dielectric properties [24].

The behavior of dielectric breakdown field (E_B) of films deposited with $R = 2.5$, as a function of the applied RF power is shown in Fig. 8. In our measurements, dielectric breakdown is defined to occur when the current through the insulator reaches 1 mA, i.e., the current density rises above 0.3 $\mathrm{A/cm}^2$. We observe from the main plot of Fig. 8 that the dielectric breakdown field increases with the RF power with a certain tendency to saturation. This trend is supported by the lowering of the hydrogen containing bonds in the films, in particular Si–H bonds, which are reported to be the main cause of electrical integrity loss in metal–insulator–semiconductor devices. The inset of Fig. 8 shows that for films deposited at 30 W, E_B decreases slightly as R increases from 2.5 to 10. This is consistent with the absence of Si–H bonds in the IR spectrum of samples with $R = 5.0$ and 10.0, and the increment in the content of N–H bonds of these samples, compared with the film deposited with $R = 1$ (see Fig. 2). The electrical properties of the film deposited at 30 W and $R = 1$, were not analyzed because its bonding configuration does not even meet those of a silicon nitride film (see Fig. 2).

The electrical (DC) conductivity, defined in terms of the value of the current density at a field strength of 1 MV/cm, was about $5\times10^{14}\ \Omega\,\mathrm{cm}$ for most of our films. This value agrees well with many reports for PECVD silicon nitride films available in the literature for the a-SiN_x used in TFT structures films [20,34,35].

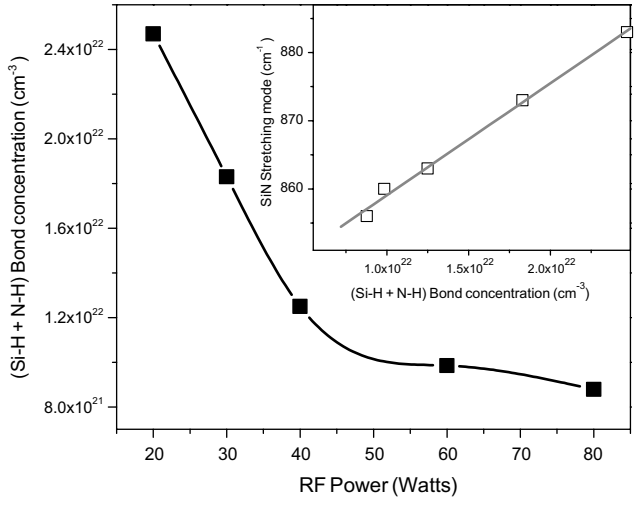

Fig. 7. Hydrogen-atom concentration (Si–H and N–H bonds) as a function of RF power. The inset shows the variation of the Si–N stretching mode frequency as a function of Si–H + N–H bonds concentration.

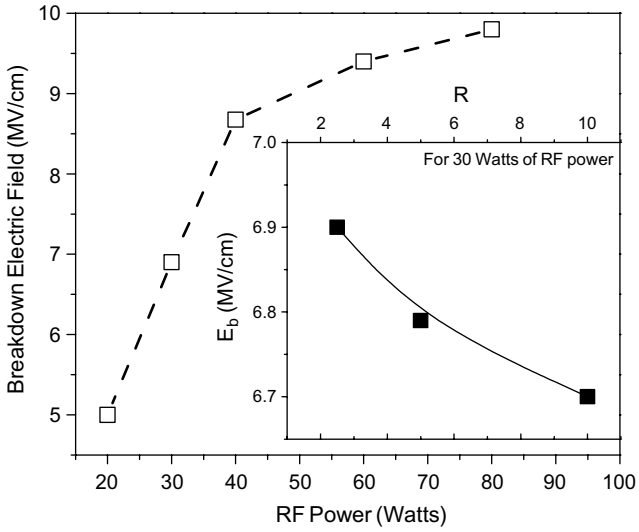

Fig. 8. Dielectric breakdown field (E_B) versus RF power. The NH_3/SiH_2Cl_2 ratios was 2.5. The inset shows that for samples deposited with 30 W, there is only a small decrease in E_B as R increases.

4. Conclusions

Silicon nitride films with a low hydrogen content have been deposited at low temperature (250 °C) by the conventional parallel-plate PECVD method from SiH_2Cl_2/NH_3/Ar mixtures. We have found that for depositions at constant power (30 W) the concentration of N–H bonds decreases as the $R = NH_3/SiCl_2H_2$ flow rates ratio decreases from 10 to 2.5, although some Si–H bonds remain incorporated in the film under this conditions. The decrease of R in this range produces a slight increase in both, the refractive index (from 1.726 to 1.82) and deposition rate (12–16.5 nm/min) of the films. However, further decrease in this ratio (until 1.0), increases drastically the N–H bonds concentration and the refractive index, and also rises the deposition rate.

For films deposited with $R = 2.5$, according to the FTIR measurements, the Si–H and N–H bonds concentrations decrease as the RF power increases, and the Si–H bonds tends to disappear at RF power values above 60 W. This hydrogen content reduction is accompanied by increments in the deposition rate and refractive index. No evidence of chlorine was found in the films, in the whole range of the experimental parameters used. In general, these silicon nitride films show high values of dielectric breakdown field (5–9 MV/cm) similar to that of stoichiometric Si_3N_4 nitrides and low values of conductivity ($<5 \times 10^{-13}\,(\Omega\,\mathrm{cm})^{-1}$). All the films were chemically stable after being immersed in water during 170 h.

Acknowledgements

The authors wish to acknowledge the technical support of J. Camacho, S. Jiménez and M.A. Canseco from the IIM-UNAM, R. Macias from the Instituto de Física-UNAM and R. Ortega from Facultad de Ciencias-UNAM. This research has been supported in part by PAPIIT-UNAM, under the extraordinary projects, IX119904 and IX107104.

References

[1] S.M. Sze, Physics of Semiconductor Devices, 2nd Ed., John Wiley, 1981.
[2] S.M. Sze, VLSI Technology, 2nd Ed., McGraw-Hill International, 1988, p. 260.
[3] H. Treichel, R. Braun, Z. Gabric, O. Spindler, A. Gschwandtner, J. Phys. II 1 (1991) 839.
[4] G. Lucovsky, J.C. Phillips, J. Non-Cryst. Solids 266–269 (2000) 1335.
[5] Y.B. Park, S.W. Rhee, J. Mater. Sci.: Mater. Electron. 12 (2001) 515.
[6] R.B. Beck, M. Giedz, A. Wojtkiewicz, A. Kudla, A. Jacubowski, Vacuum 70 (2003) 323.
[7] I.K. Naik, Proc. Soc. Photo-Opt. Instrum. Eng. 460 (1984) 56.
[8] M.J. Rand, R.D. Standley, Appl. Opt. 11 (1972) 2482.
[9] K.E. Mattsson, J. Appl. Phys. 77 (1995) 6616.
[10] G. Santana, A. Morales-Acevedo, Sol. Energy Mater. Sol. Cells 60 (2000) 135.
[11] L.S. Zambom, R.D. Mansano, R. Furlan, P. Verdonck, Thin Solid Films 343&344 (1999) 299.
[12] G. Beshkov, S. Lei, V. Lazarova, N. Nedev, S.S. Georgiev, Vacuum 69 (2003) 301.
[13] G. Bruno, P. Capezzuto, A. Madan (Eds.), Plasma Deposition of Amorphous Silicon-based Materials, Academic, Boston, 1995.
[14] G. Lucovsky, IBM J. Res. Develop. 43 (1999) 301.
[15] C.Y. Chang, S.M. Sze, ULSI Technology, Wiley International, New York, 2000.
[16] C. Hodson, Plasma Technol. Process Newslett.-OIPT (January) (2004) 4.
[17] J.C. Barbour, H.J. Stein, O.A. Popov, M. Yoder, C.A. Outten, J. Vac. Sci. Technol., A 9 (1991) 480.
[18] C. Doughty, D.C. Knick, J.B. Bailey, J.E. Spencer, J. Vac. Sci. Technol., A 17 (1999) 2612.
[19] G. Lucovsky, D. Tsu, J. Cryst. Growth 86 (1988) 804.
[20] L.D. Zambom, R.D. Mansano, Vacuum 71 (2003) 439.
[21] Y. Kuo, H.H. Lee, Vacuum 66 (2002) 299.
[22] M. Bose, D.K. Basa, D.N. Bose, Mater. Lett. 48 (2001) 336.
[23] B. Kim, D.W. Kim, S.S. Han, Vacuum 72 (2004) 385.
[24] W.S. Liao, C.H. Lin, S.C. Lee, Appl. Phys. Lett. 65 (1994) 2229.
[25] A.C. Adams, Solid State Technol. 26 (1983) 135.
[26] F. Ay, A. Aydinli, Opt. Mater. 26 (2004) 33.
[27] D.V. Tsu, G. Lucovsky, M.J. Mantini, Phys. Rev. B 33 (1986) 7069.
[28] D.V. Tsu, G. Lucovsky, J. Vac. Sci. Technol., A 4 (1986) 480.
[29] N.M. Park, S.H. Choi, S.J. Park, Appl. Phys. Lett. 81 (2002) 1092.
[30] M.B. Robinson, A.C. Dillon, S.M. George, J. Vac. Sci. Technol. 13 (1995) 35.
[31] G. Bruno, P. Capezzuto, G. Cicala, F. Cramarossa, J. Appl. Phys. 62 (1987) 2050.
[32] V.M. Donnelly, M.V. Malyshev, M. Schabel, A. Kornblit, W. Tai, I.P. Herman, N.C.M. Fuller, Plasma Sources Sci. Technol. 11 (2002) A26.
[33] W.A. Lanford, M.J. Rand, J. Appl. Phys. 49 (1978) 2473.
[34] I. Atilgan, S. Ozder, O. Ozdemir, B. Katircio, J. Non-Cryst. Solids 249 (1999) 131.
[35] S. Bae, D.G. Farber, S.J. Fonash, Solid-State Electron. 44 (2000) 1355.